Langmuir

Article

pubs.acs.org/Langmuir

Mixed Diacetylene/Octadecyl Melamine Nanowires Formed at the Air/Water Interface Exhibit Unique Structural and Colorimetric Properties

Hao Jiang and Raz Jelinek*

Department of Chemistry and Ilse Katz Institute for Nanotechnology, Ben Gurion University of the Negev, Beer Sheva 84105, Israel

Supporting Information

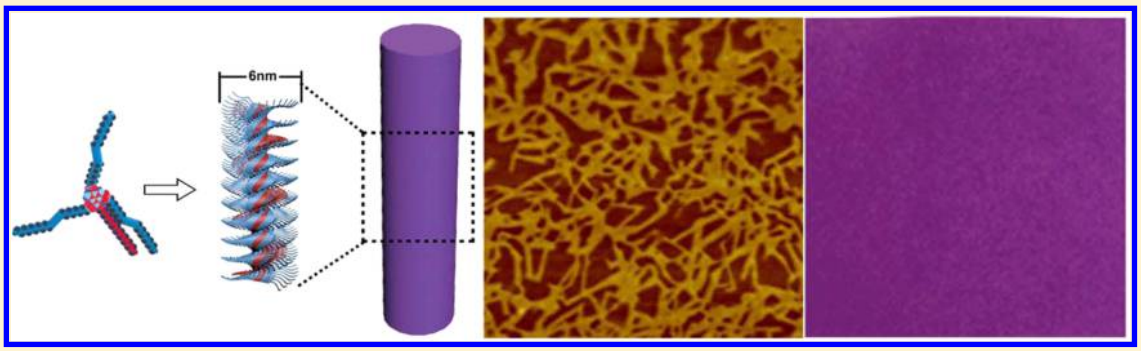

ABSTRACT: Polydiacetylene (PDA) assemblies exhibit interesting photophysical properties, specifically, visible colorimetric transformations. A considerable body of work has focused on the formation and characterization of PDA Langmuir monolayer systems, and the overwhelming majority of reports so far have indicated that the adoption of 2D sheetlike structures associated with a hydrogen bond network between the diacetylene headgroups is a prerequisite for polymerization and chromatic properties. Here we report for the first time on the assembly of nanowire networks in mixed Langmuir monolayers comprising diacetylene monomers and octadecyl melamine surfactants. Structural and physical analysis indicates that the nanowires are composed of a helical organization of stacked diacetylene/octadecyl melamine building blocks assembled through hydrogen bonds between the melamine residues and the carboxylic termini of the diacetylenes. Following ultraviolet-induced polymerization, the PDA/octadecyl melamine nanowires exhibited unusual chromatic properties, specifically, an absence of the ubiquitous "blue" phase, rather transforming into a new "purple" PDA phase. This study demonstrates that the incorporation of surfactant constituents within diacetylene frameworks provides a means for modulating the structural and chromatic features of PDA assemblies, giving rise to new morphologies and unique optical properties.

INTRODUCTION

Polydiacetylenes (PDAs) are quasi-1D π-conjugated polymers displaying interesting structural and optical properties.[1−6] In recent years, these polymers have attracted considerable interest both scientifically and as promising sensing platforms, primarily because of their visible color transformations induced by a variety of external perturbations, such as heat,[7] organic solvents,[8] mechanical stress,[9] ligand−receptor interactions,[10−12] and others. The intriguing chromatic properties of PDA assemblies arise from the ene−yne topo-polymerization, made possible through self-assembly of the diacetylene monomers.[13] While most studies of PDA systems have focused on vesicular or sheetlike configurations, diverse PDA nanostructures have also been reported, including nanorods,[14] nanowires,[15] and helical nanoribbons.[16] The underlying morphologies of diacetylene assemblies are determined by varied intermolecular forces, primarily hydrogen bonding between the diacetylene headgroups and hydrophobic interactions involving the alkyl moieties.[13−16]

Because diacetylenes contain extended alkyl chains, they form Langmuir monolayers upon deposition at the air/water interface. Many studies have investigated diacetylenes and their polymerized framework—polydiacetylenes—at the air/water interface, including their thermodynamic profiles,[17,18] structural and photophysical properties,[19−21] and potential practical applications.[2,4,22] An almost universal structural feature of PDA systems in Langmuir monolayer environments is the formation of sheetlike lamellar organizations that make possible polymerization and the formation of a chromatic conjugated system.[23,24]

Here we explore the unique structural and chromatic properties of mixed Langmuir monolayers comprising diacetylene monomer 10,12-tricosadiynoic acid (TrCDA) and surfactant octadecyl melamine (OM). OM has been previously shown to adopt interesting self-assembled structures at the air−water interface.[25,26] OM also formed disklike structures

Received: March 11, 2015
Published: May 13, 2015

DOI: 10.1021/acs.langmuir.5b01697
Langmuir 2015, 31, 5843−5850

assembled through hydrogen bond interactions with carboxylic acids.[27] Interestingly, we report here that the isothermal compression of diacetylene/OM monolayers at the air/water interface gave rise to the formation of nanowires. Structural analysis indicate that the nanowires comprise both diacetylenes and OM, held together through hydrogen bonding between the amine protons of the melamine ring and the carboxylic residues of TrCDA. Importantly, the new diacetylene/OM nanowires displayed unique chromatic properties, specifically, a new polydiacetylene "purple phase". This work demonstrates that mixing diacetylene monomers with surfactant molecules expands the structural and chromatic universe of polydiacetylene systems, opening new avenues for modulating the photophysical properties of the polymer.

MATERIALS AND METHODS

Materials. Diacetylene monomer 10,12-tricosadiynoic acid (TrCDA) was purchased from Alfa Aesar. 2-Chloro-4,6-diamino-1,3,5-triazine, octadecylamine, and anhydrous sodium hydrogen carbonate were purchased from Sigma-Aldrich and were used as received. Octadecyl melamine (OM) was synthesized according to published procedures.[27] Briefly, a mixture of 2-chloro-4,6-diamino-1,3,5-triazine (19 mmol), octadecylamine (19 mmol), and anhydrous sodium hydrogen carbonate (19 mmol) in 1,4-dioxan (75 mL) was refluxed under an argon atmosphere for 6 h. The reaction mixture was then cooled and poured into water (100 mL). The precipitate was filtered off and washed with water. The product was purified by flash chromatography on silica gel and eluted with a dichloromethane/methanol 10:1 mixture.

Langmuir Film Preparation and Analysis. Langmuir monolayer measurements were performed using a computerized Langmuir trough (model 622/D1, Nima Technology Ltd., Coventry, U.K.) at 25 °C. The TrCDA/OM mixtures were obtained after evaporating chloroform solutions of OM and TrCDA in predetermined mole ratios by stirring at room temperature. The assemblies were subsequently redissolved in chloroform to a total concentration of 1 mg·mL^{-1} and spread onto the water surface. After the evaporation of the organic solvent and Langmuir monolayer formation, the barriers of the trough were compressed at a rate of 10 cm^2·min^{-1}. Monolayers were transferred onto hydrophobic silica wafers by the horizontal Langmuir–Schaefer (LS) or vertical Langmuir–Blodgett method, depending upon the experiments desired.

Ex-Situ Characterization. Proton NMR spectra were acquired on Bruker 500 MHz spectrometers. ^{1}H NMR data were acquired in $CDCl_3$, and the temperature was controlled at 298 K. Atomic force microscopy (AFM) images were recorded under ambient conditions on monolayers transferred through the LS method in tapping mode using a Digital Instruments Dimension 3100 mounted on an active antivibration table. Transmission electron microscopy (TEM) experiments were carried out on an FEI Tecnai 12 G2 TWIN TEM at an acceleration voltage of 120 kV. Images were recorded on a 1k × 1k CCD camera (Gatan model 794). The samples were prepared on 400-mesh copper Formvar/carbon grids with the LS method. Circular dichroism (CD) spectra of all LB films of up to 80 layers on glass substrates were recorded in the range of 400–800 nm at room temperature on a Jasco J-715 spectropolarimeter. X-ray diffraction (XRD) spectra were obtained using a PANalytical's Empyrean thin film diffractometer equipped with a parabolic mirror on the incident beam providing quasi-monochromatic Cu Kα radiation (λ = 1.54059 Å) and an X'Celerator linear detector. Langmuir–Blodgett films of up to 80 layers were deposited on a hydrophilic silica wafer for XRD measurement. Visible spectra of all LB films of up to 80 layers on glass substrates were carried out using a Jasco V-550 UV/vis spectrophotometer. Raman measurements were performed on a Jobin-Yvon LabRam HR 800 micro-Raman system, equipped with a liquid-nitrogen-cooled detector. The excitation source was an argon laser (514 nm) with a power of 5 mW on the sample. To protect the samples the laser power was reduced by 1000-fold using ND filters. The laser was focused with a 100× long-focal-length objective to a spot of about 4 μm. Measurements were taken with the 600 grating per mm and a microscope confocal hole setting of 100 μm with a typical exposure time of 1 min.

RESULTS AND DISCUSSION

Figure 1 depicts the molecular structures of the diacetylene monomer (10,12-tricosadiynoic acid, TrCDA) and octadecyl

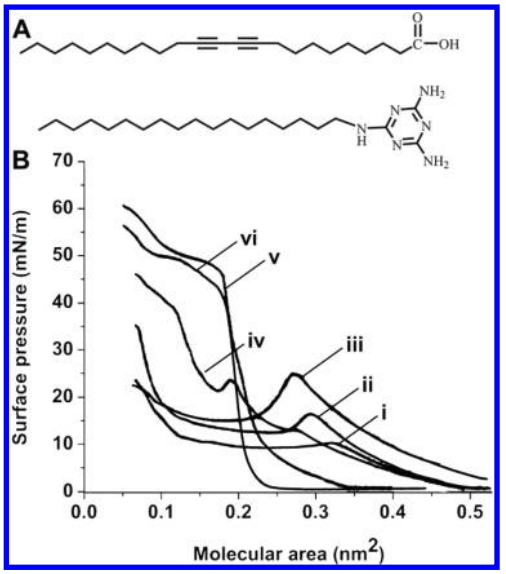

Figure 1. Thermodynamic profiles of mixed diacetylene/octadecyl melamine Langmuir monolayers. (A) Molecular structures of diacetylene monomer TrCDA (top) and OM (bottom). (B) Surface pressure/area isotherms of mixed TrCDA/OM Langmuir monolayers at different mole ratios between the two components: TrCDA/OM mole ratios of 6:1 (ii), 3:1 (iii), 1:1 (iv), and 1:3 (v) as well as pure TrCDA (i) and OM (vi).

melamine (OM) and surface-area/pressure isotherms recorded for Langmuir monolayers having different mole ratios between the two components. All isotherms exhibit pressure collapses which likely reflect multilayer formation.[28,29] However, the shapes of the compression isotherms, the molecular areas in which the collapse occurred, and the collapse surface pressures were significantly different between the different monolayers. For example, the surface pressure/area isotherm recorded for the monolayer with the highest diacetylene concentration (TrCDA/OM mole ratio of 6:1, Figure 1B,ii) resembles isotherms recorded for pure diacetylene (Figure 1B,i).[17,18] Similarly, the monolayer with the lowest TrCDA/OM mole ratio (1:3, Figure 1B,v) produced a compression isotherm that is close in appearance to pure OM (Figure 1B,vi).[25] Overall, the surface pressure/area isotherms in Figure 1B indicate pronounced interactions between the diacetylene monomers and OM in the mixed monolayers.

Nuclear magnetic resonance (NMR) spectra recorded for TrCDA/OM mixtures in chloroform (e.g., prior to deposition onto the air/water interface) reveal significant shifts of the melamine amine protons, which were dependent upon the mole ratios between the two components (Figure 2A). Specifically, the two amine peaks in a solution of pure OM appear at approximately 4.8 ppm (Figure 2A,i). However, addition of the diacetylene monomer gave rise to significant downfield shifts for the amine protons; the solution comprising a 1:1 mol ratio between OM and TrCDA displayed amine

DOI: 10.1021/acs.langmuir.5b01697
Langmuir 2015, 31, 5843–5850

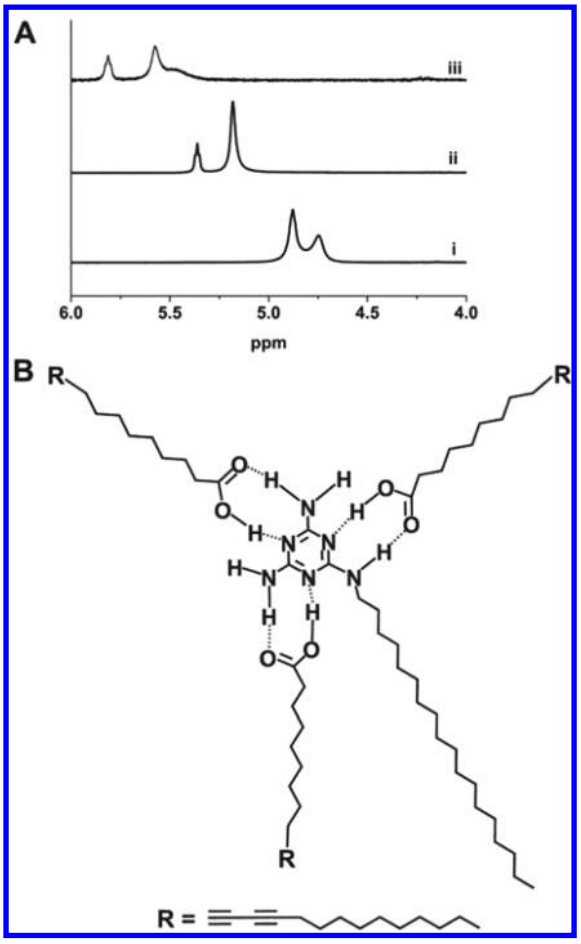

Figure 2. Hydrogen bonding between melamine and diacetylene monomers. (A) Amine proton region of the NMR spectra recorded for TrCDA/OM mixtures prior to deposition at the air/water interface: pure OM (i); 1:1 mol ratio between TrCDA and OM (ii); and 3:1 mol ratio between TrCDA and OM (iii). (B) Model for the hydrogen-bonding network assembled between melamine and three TrCDA residues.

peaks at around 5.2−5.3 ppm (Figure 2A,ii) whereas a pronounced downfield shift to between 5.6−5.8 ppm was recorded in a solution containing a 3:1 TrCDA/OM mole ratio (Figure 2A,iii).

The pronounced shifts of the OM amine protons are indicative of hydrogen bond formation between the melamine residue of OM and the diacetylene molecules.[27] Figure 2B presents a structural model showing the hydrogen bonds formed between the amine protons of melamine and the carboxylic headgroups of three diacetylene residues. Indeed, according to the model in Figure 2B, significant shifts of the NH and NH_2 OM protons are expected to occur. In particular, the most pronounced shift should be observed in the sample containing a 3:1 mol ratio between diacetylene and OM, in which six hydrogen bonds are present. A significant downfield shift is indeed apparent in the NMR spectrum of TrCDA/OM (3:1 mol ratio) in Figure 2A,iii. Furthermore, hydrogen bonding between the NH_2 moieties of melamine and TrCDA, according to the model in Figure 2B, likely accounts for the broad proton peak at around 5.5 ppm (Figure 2A,iii) because the hydrogen bond is expected to produce distinguishable environments for the two NH_2 protons.

Figure 3 presents an atomic force microscopy (AFM) analysis of monolayers prepared at different mole ratios between the diacetylene monomer and OM, horizontally transferred from the water surface at a surface pressure of 20 mN/m (i.e., the Langmuir−Schaeffer technique). Echoing the thermodynamic experiments (Figure 1) and NMR data (Figure 2), the AFM images reveal significant changes in the films' structural features that are clearly linked to the ratio between TrCDA and OM. Specifically, typical irregular diacetylene sheets[23,24] were observed in films comprising a high, 6:1 TrCDA/OM mole ratio (Figure 3A), and extended uniform films were apparent in the case of monolayers exhibiting a high concentration of OM (1:3 diacetylene/OM mole ratio, Figure 3D).[25,26] However, remarkable nanowires were observed in monolayers exhibiting intermediate TrCDA/OM mole ratios (Figure 3B,C). In particular, while few nanowires were observed in the AFM image of a Langmuir monolayer comprising a 3:1 TrCDA/OM mole ratio (Figure 3B), a dense nanowire network emerged upon compression of a monolayer containing equimolar concentrations of OM and diacetylene (Figure 3C). The nanowires were randomly dispersed albeit they exhibited a relative uniform height of approximately 6 nm, apparent in the height profiles included in Figure 3B,C. The relationship between the relative abundance of nanowires in the Langmuir monolayers and the diacetylene/OM mole ratio indicates that the nanowires likely comprise both OM and the diacetylene monomers.

To further characterize the structural features and organization of the TrCDA/OM nanowires, we carried out transmission electron microscopy (TEM, Figure 4A) and circular dichroism (CD, Figure 4B) experiments. Both experiments seem to indicate an intriguing helical organization of the TrCDA/OM units within the nanowires. Specifically, the TEM images in Figure 4A reveal distinct helical pitches within the nanowires. The CD spectra in Figure 4B further confirm that the TrCDA/OM films exhibit supramolecular chirality that is directly traced to helical conformations of the nanowires, consistent with previous work on supramolecular chirality at the air−water interface.[30,31] Specifically, it has been shown that the supramolecular chirality of polydiacetylene LB films is related to symmetry breaking at the interface induced upon compression, even though the monomers themselves are achiral.[30,31] Furthermore, it should be noted that opposite CD polarities could be obtained in different batches as shown in Figure 4B because the overall handedness (e.g., pitch direction) of the nanowire is determined by the directionality of the initial nucleating aggregate, which is formed randomly upon compression of the monolayer at the air/water interface.[31]

The formation of nanowires such as recorded in the AFM and TEM experiments (Figures 3 and 4, respectively) can be explained according to the structural model outlined in Figure 5. Figure 5 depicts the space-filling model of the TrCDA/OM unit assembled via the hydrogen-bond network between the melamine headgroup and terminal carboxylic acid residues of three diacetylene monomers (e.g., Figure 2B). The hydrogen-bonded diacetylene/OM unit constitutes the building block of the nanowires, which are essentially assembled through stacking the melamine rings upon each other (Figure 5B), akin to the widely reported π-stacking organization in biological and synthetic nanowire morphologies containing aromatic rings.[32,33] Notably, the calculated diameter of the diacetylene/OM backbone unit, based upon the dimensions of the circle traced by the diacetylene side-chain residue, is approximately 6

DOI: 10.1021/acs.langmuir.5b01697
Langmuir 2015, 31, 5843−5850

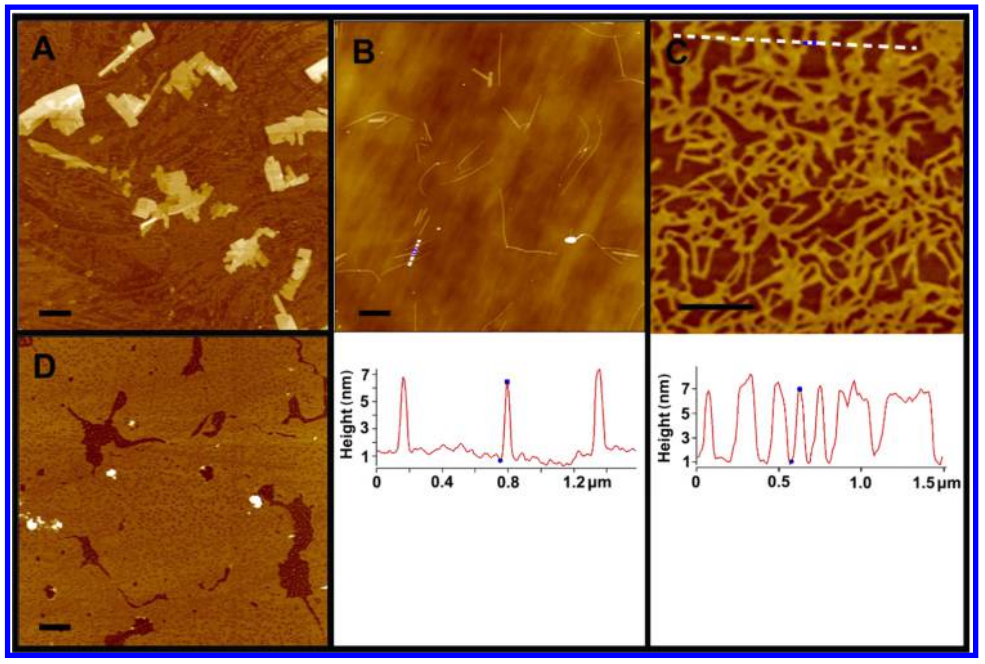

Figure 3. Atomic force microscopy (AFM) analysis of mixed diacetylene/OM Langmuir monolayers. Monolayers were transferred at a surface pressure of 20 mN/m. (A) 6:1 TrCDA/OM mole ratio; the scale bar is 2 μm. (B) 3:1 mol ratio; the scale bar is 2 μm. (C) 1:1 mol ratio; the scale bar is 0.5 μm. (D) 1:3 mol ratio; the scale bar is 2 μm. The height profiles (cross sections) are included in B and C, extracted along the broken white line indicated in the images.

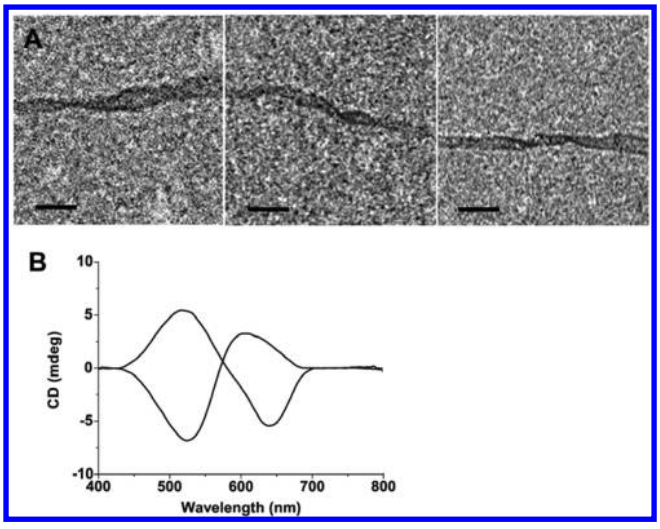

Figure 4. Helical organization of the TrCDA/OM nanowires. (A) Transmission electron microscopy (TEM) images showing TrCDA/OM nanowires; the helical pitches are apparent. Scale bars correspond to 50 nm. (B) Circular dichroism (CD) spectra of TrCDA films transferred from the air/water interface. The film chirality gave rise to CD signals (two polarizations recorded for two film samples).

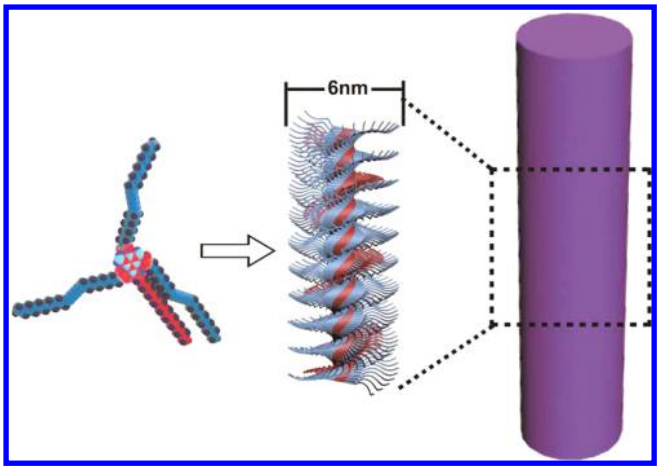

Figure 5. Structural model for the assembly of diacetylene/octadecyl melamine nanowires. Space-filling model on the left showing the hydrogen-bonded diacetylene/OM unit. The diacetylene/OM building blocks are stacked through $\pi-\pi$ interactions, forming the backbone of the nanowire on the right.

nm, consistent with the AFM measurements in Figure 3B,C. The assembly mechanism can be explained according to the following mechanism: upon initial spreading on the water subphase, the hydrophilic domains of the TrCDA/OM units insert into the water subphase while the alkyl chains extend toward the air. Subsequent isothermal compression leads to the assembly of the nanowires, promoted by π stacking between the melamine moieties. A similar model was proposed in a recent study of alkyl-functionalized hydrophilic molecular "disks".[34]

The model depicted in Figure 5 which points to the formation of nanowires through the organization of three diacetylene monomers around a central (single) melamine moiety supported by the hydrogen-bond network raises the question as to why a significantly denser nanowire network was recorded in the compressed Langmuir monolayer comprising a 1:1 mol ratio between TrCDA and OM (AFM image in Figure 3C). It is likely, however, that not all TrCDA/OM units incorporate within the nanowires, particularly at lower surface pressures. Importantly, both the compression isotherm analysis (Figure 1) and AFM experiments (Figure 3) indicate that the transformation of the mixed monolayer into a condensed phase is a requisite for nanowire formation.

DOI: 10.1021/acs.langmuir.5b01697
Langmuir 2015, 31, 5843−5850

In this context, the compression isotherms in Figure 1 clearly show that at the surface pressure of 20 mN/m (corresponding to a condensed monolayer phase) the molecular area of the monolayer comprising a ratio of 1:1 between TrCDA and OM is smaller than that of the monolayer having a 3:1 ratio between TrCDA and OM (curves 1B,iii and 1B,ii, respectively). This result means that the TrCDA/OM (1:1 ratio) monolayer is more condensed than the TrCDA/OM (3:1 ratio). Accordingly, because OM promotes the formation of a condensed phase, a higher concentration of OM within the monolayer (e.g., higher ratio between OM and TrCDA) led to a greater abundance of nanowires (e.g., Figure 3C). Corroborating this interpretation was the observation that when the TrCDA:OM (3:1) monolayer was transferred onto a solid substrate at a higher surface pressure (40 mN/m) we recorded a much denser distribution of nanowires (new Figure S1).

To confirm the structural model outlined in Figure 5 and to further elucidate the structural features of the diacetylene/OM nanowires, we carried out X-ray diffraction (XRD) experiments, examining films with different diacetylene/OM mole ratios (Figure 6). The XRD analysis utilized multilayer films, extracted onto a solid substrate through consecutive vertical transfers (i.e., the Langmuir–Blodgett technique, specifically, the film samples inspected in Figure 6 composed of 80 vertical transfer cycles). The XRD data in Figure 6 echo the structural evolution of the diacetylene/OM assemblies apparent in the AFM experiments (Figure 3). The XRD peak corresponding to a *d* spacing of 4.26 nm ascribed to pure diacetylene lamellae[35] was recorded in films comprising only diacetylene (Figure 6A). A small trace of this *d* spacing was still apparent in a film comprising a 3:1 mol ratio between the diacetylene monomer and OM (Figure 6B), while a distinctive prominent *d* spacing of 5.98 nm appeared in the XRD pattern recorded for this film. Indeed, the diffraction peak corresponding to 5.98 nm became the sole feature in the XRD spectrum of the 1:1 diacetylene/OM film (Figure 6C). Notably, the XRD peak corresponding to a *d* spacing of 5.98 nm matches both the nanowire diameter observed in the AFM experiments (Figure 3B,C) and the calculated diameter of the hydrogen-bonded diacetylene/OM unit (Figure 5). As such, the XRD analysis provides evidence for the structural model in Figure 5, according to which the hydrogen-bonded diaetylene/OM units constitute the building blocks of the nanowires.

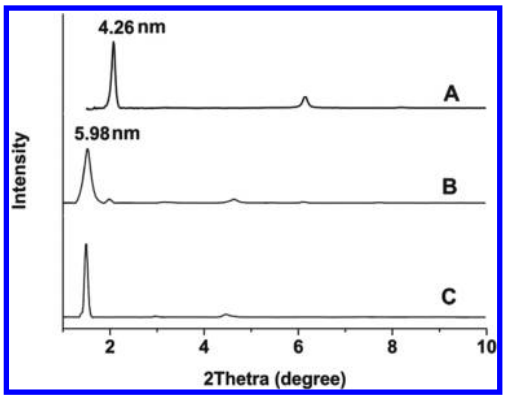

Figure 6. X-ray diffraction (XRD) patterns of diacetylene/octadecyl melamine films. (A) Pure TrCDA film. (B) TrCDA/OM (3:1 mol ratio). (C) TrCDA/OM (1:1 mol ratio).

To decipher the significance of isothermal compression in nanowire formation at the air/water interface, we examined TrCDA/OM films prepared through spin coating on silicon wafers (Figure S2). The representative AFM images depicted in Figure S2 demonstrate that short nanorods and irregular aggregates rather than elongated nanowires were the predominant features in the spin-coated films. Similarly, AFM analysis of monolayers transferred from the air/water interface at a low surface pressure of 5 mN/m highlights the formation of abundant small aggregates and short rods. Moreover, these nanostructures were "soft" and readily attached to the AFM tip, consistent with less rigidity that is likely associated with the lower surface pressure exerted. These observations confirm that the isothermal compression of the TrCDA/OM mixture is key to nanowire assembly.

The diacetylene/OM nanowire films exhibit unique photophysical properties (Figures 7 and 8). Figure 7 compares the visual appearance and ultraviolet–visible spectra of a pure diacetylene film and a diacetylene/OM film containing a 1:1 mol ratio of the two molecules. Both films were polymerized through irradiation with ultraviolet light (254 nm), and their colorimetric properties were examined. UV irradiation induces the polymerization of organized diacetylene networks, forming polydiacetylene (PDA) which usually exhibits a blue appearance.[6,7] Extended UV irradiation also gives rise to the colorimetric transformations (in most cases blue to red) of PDA.[36,37] The scanned images of the films exposed to different durations of UV irradiation in Figure 7 demonstrate significant differences in film color and visual appearance between the two film compositions.

Specifically, similar to previous reports,[36,37] the pure PDA film appeared to be blue following short UV irradiation and was transformed to a purple color after a longer irradiation time (Figure 7A). The diacetylene/OM (1:1 mol ratio) nanowire film, in contrast, did not exhibit the blue phase after short UV irradiation but rather appeared to be light purple (Figure 7B). Furthermore, an extended 40 min of irradiation of the PDA/OM film gave rise to a uniform purple-red film (Figure 7B) which was markedly different than the nonhomogeneous purple film observed in the case of 40 min of UV irradiation of pure PDA (Figure 7A). The uniform appearance of the PDA/OM film can be traced to the multilayered feature, as the film was formed through the Langmuir–Blodgett technique (using 80 transfer cycles). Accordingly, the resultant dense nanowire network produced a visibly uniform film on a rather macroscopic scale, as shown in Figure 7B.

The visible absorbance spectra in Figure 7C,D further underscore the distinctive colorimetric properties of the PDA/OM films. The visible spectra clearly show that the PDA/OM film did not transform into the initially irradiated blue phase, ubiquitous in numerous reported PDA systems. Specifically, whereas the blue appearance of the pure PDA film is reflected in the prominent absorbance at around 650 nm (Figure 7C), this absorbance peak was significantly attenuated in the PDA/OM film (Figure 7D). Rather, initial short irradiation of 12 s produced a unique purple phase, exhibiting broader absorbance at around 600–620 nm (Figure 7D). It should be emphasized that even irradiation times that were shorter than 12 s did not produce a blue PDA (data not shown). Moreover, the spectra in Figure 7D demonstrate that upon longer irradiation times the absorbance of the PDA/OM film was significantly shifted to lower wavelengths as compared to the visible absorbance of

DOI: 10.1021/acs.langmuir.5b01697
Langmuir 2015, 31, 5843–5850

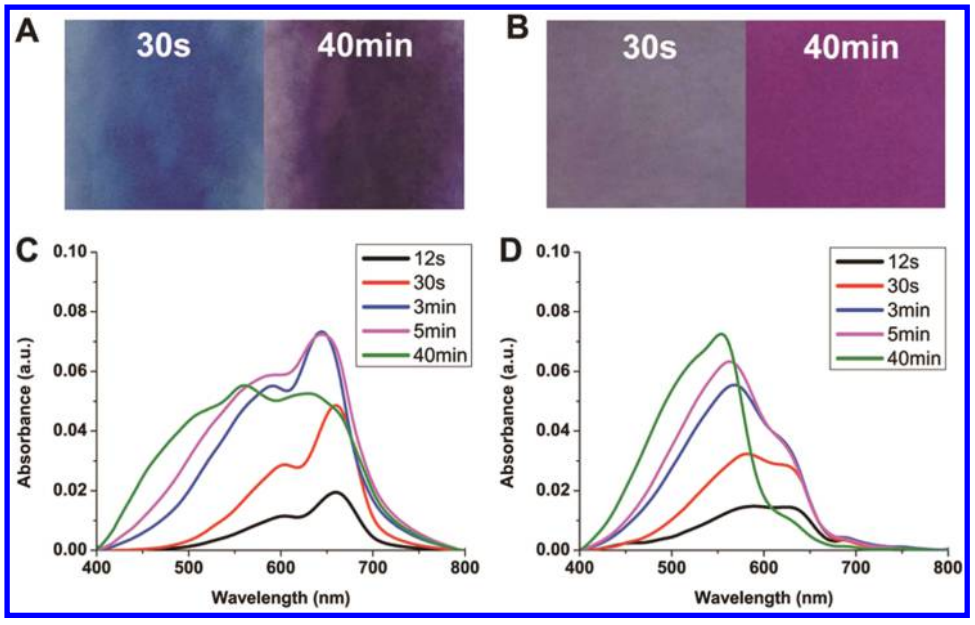

Figure 7. Color properties of polydiacetylene/octadecyl melamine films. (A) Scanned images of a pure PDA film following the indicated irradiation times. (B) Scanned images of a PDA/OM film (1:1 mol ratio) following the indicated irradiation times. (C) Visible absorbance spectra of a pure PDA film following UV irradiation for the indicated durations. (D) Visible absorbance spectra of the PDA/OM film (1:1 mol ratio) following UV irradiation for the indicated durations. The films were obtained through the Langmuir–Blodgett technique using 80 transfer cycles.

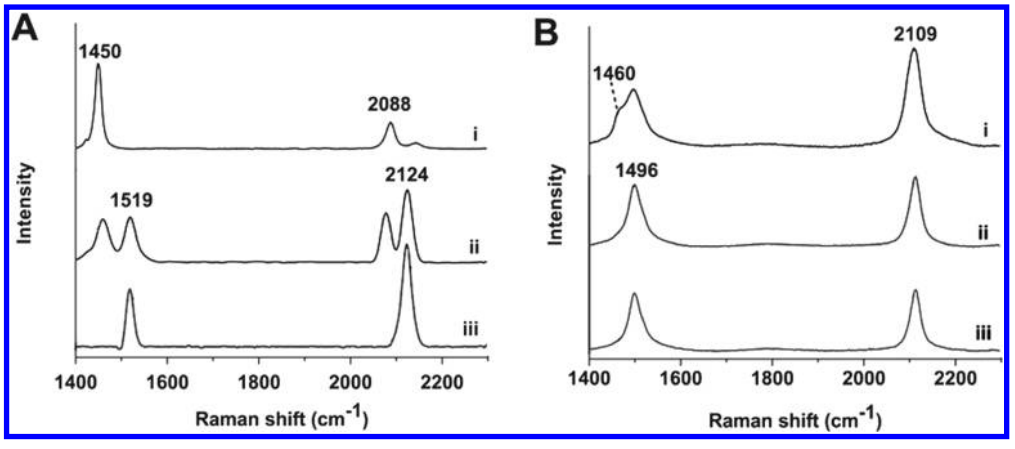

Figure 8. Raman scattering peaks in the conjugated alkyne–alkene spectral region of (A) a pure PDA film and (B) a diacetylene/OM film (1:1 mol ratio). (i) UV irradiation for 30 s. (ii) UV irradiation for 40 min. (iii) Heating to 70 °C for 30 min.

pure PDA, accounting for the more pronounced purple-red appearance of the PDA/OM film (e.g., Figure 7B).

Raman scattering analysis in Figure 8 provides additional complementary evidence for a distinctive PDA purple phase associated with the PDA/OM nanowires. The Raman scattering data in Figure 8 show the Raman spectral region corresponding to the conjugated alkyne–alkene groups and compare the structural features of the PDA/OM nanowire film and a pure PDA film in different polymerization stages (e.g., different irradiation times). The purePDA film gave rise initially to the typical blue-phase Raman signals at around 1450 and 2088 cm^{-1} (Figure 8A,i).[36,38] Distinct peaks corresponding to red-phase PDA appeared at approximately 1519 and 2124 cm^{-1} following extended UV irradiation for 40 min (Figure 8A,ii). These Raman signals became the sole spectral features after heating (Figure 8A,iii), corresponding to fully transformed PDA to the red phase.[31]

The Raman spectra of the diacetylene/OM nanowire film (1:1 mol ratio) in Figure 8B were significantly different from those of the pure PDA film. Specifically, short UV irradiation (30 s) of the mixed film produced a distinctive Raman signal at around 1496 cm^{-1} with a small shoulder at 1460 cm^{-1} (Figure 8B,i). The peak at around 1496 cm^{-1} became the predominant spectral feature upon extended (40 min) UV irradiation (Figure 8B,ii) and heating (Figure 8B,iii). To the best of our knowledge, the Raman scattering signal at 1496 cm^{-1} has not been previously reported and correlates with the formation of the new purple-red PDA phase apparent in the colorimetric analysis in Figure 7.

■ CONCLUSIONS

The unique colorimetric properties of polydiacetylene (PDA) systems, a core feature of these remarkable conjugated polymers, are intimately dependent upon the structural organization and morphologies of the diacetylene assemblies. As such, creating new PDA configurations could open the way to manipulations of the photophysical properties of the polymer. This study demonstrates the assembly of a nanowire

DOI: 10.1021/acs.langmuir.5b01697
Langmuir 2015, 31, 5843–5850

network through the isothermal compression of mixed Langmuir monolayers comprising diacetylene monomers and octadecyl melamine surfactants. Structural analysis and molecular modeling indicate that the nanowires comprise both molecular constituents and that the intriguing helical nanowire morphology is ascribed to hydrogen bonding between the melamine residue and the carboxylic moieties of the diacetylenes. Interestingly, the diacetylene/OM nanowires display unique chromatic properties, specifically, a new polydiacetylene purple phase, apparent in both visible absorbance spectral analysis and the Raman scattering experiments. This work demonstrates that new PDA morphologies exhibiting unique chromatic properties can be generated through the compression of mixed surfactant/diacetylene assemblies at the air/water interface.

■ ASSOCIATED CONTENT

Supporting Information

AFM image of a TrCDA/OM (3:1) monolayer transferred onto a solid substrate at a higher surface pressure of 40 mN/m. AFM images of mixed diacetylene/OM films with spin-coating of the chloroform solutions. AFM images of mixed diacetylene/OM Langmuir monolayers at a lower surface pressure of 5 mN/m. The Supporting Information is available free of charge on the ACS Publications website at DOI: 10.1021/acs.langmuir.5b01697.

■ AUTHOR INFORMATION

Corresponding Author

*E-mail: razj@bgu.ac.il.

Notes

The authors declare no competing financial interest.

■ ACKNOWLEDGMENTS

We are grateful to the US−Israel BARD Foundation for financial support. H.J. acknowledges the China−Israel Postdoctoral Support grant program.

■ REFERENCES

(1) Wegner, G. Topochemical reactions of monomers with conjugated triple bonds.i. polymerization of 2.4-hexadiyn-1.6-diols deivatives in crystalline state. *Z. Naturforsch., B* **1969**, *24*, 824.

(2) Reppy, M. A.; Pindzola, B. A. Biosensing with polydiacetylene materials: structures, optical properties and applications. *Chem. Commun.* **2007**, 4317−4338.

(3) Ahn, D. J.; Kim, J. M. Fluorogenic polydiacetylene supramolecules: Immobilization, micropatterning, and application to label-free chemosensors. *Acc. Chem. Res.* **2008**, *41*, 805−816.

(4) Sun, X. M.; Chen, T.; Huang, S. Q.; Li, L.; Peng, H. S. Chromatic polydiacetylene with novel sensitivity. *Chem. Soc. Rev.* **2010**, *39*, 4244−4257.

(5) Yarimaga, O.; Jaworski, J.; Yoon, B.; Kim, J. M. Polydiacetylenes: supramolecular smart materials with a structural hierarchy for sensing, imaging and display applications. *Chem. Commun.* **2012**, *48*, 2469−2485.

(6) Xu, Q.; Lee, S.; Cho, Y.; Kim, M. H.; Bouffard, J.; Yoon, J. Polydiacetylene-Based Colorimetric and Fluorescent Chemosensor for the Detection of Carbon Dioxide. *J. Am. Chem. Soc.* **2013**, *135*, 17751−17754.

(7) Kauffman, J. S.; Ellerbrock, B. M.; Stevens, K. A.; Brown, P. J.; Pennington, W. T.; Hanks, T. W. Preparation, Characterization, and Sensing Behavior of Polydiacetylene Liposomes Embedded in Alginate Fibers. *ACS Appl. Mater. Interfaces* **2009**, *1*, 1287−1291.

(8) Jiang, H.; Wang, Y. L.; Ye, Q.; Zou, G.; Su, W.; Zhang, Q. J. Polydiacetylene-based colorimetric sensor microarray for volatile organic compounds. *Sens. Actuators B* **2010**, *143*, 789−794.

(9) Park, D. H.; Hong, J.; Park, I. S.; Lee, C. W.; Kim, J. M. A Colorimetric Hydrocarbon Sensor Employing a Swelling-Induced Mechanochromic Polydiacetylene. *Adv. Funct. Mater.* **2014**, *24*, 5186−5193.

(10) Wu, J. C.; Zawistowski, A.; Ehrmann, M.; Yi, T.; Schmuck, C. Peptide Functionalized Polydiacetylene Liposomes Act as a Fluorescent Turn-On Sensor for Bacterial Lipopolysaccharide. *J. Am. Chem. Soc.* **2011**, *133*, 9720−9723.

(11) de Oliveira, T. V.; Soares, N. D. F.; Silva, D. J.; de Andrade, N. J.; Medeiros, E. A. A.; Badaro, A. T. Development of PDA/Phospholipids/Lysine vesicles to detect pathogenic bacteria. *Sens. Actuators B* **2013**, *188*, 385−392.

(12) Banerjee, S.; Konig, B. Molecular Imprinting of Luminescent Vesicles. *J. Am. Chem. Soc.* **2013**, *135*, 2967−2970.

(13) Tanioku, C.; Matsukawa, K.; Matsumoto, A. Thermochromism and Structural Change in Polydiacetylenes Including Carboxy and 4-Carboxyphenyl Groups as the Intermolecular Hydrogen Bond Linkages in the Side Chain. *ACS Appl. Mater. Interfaces* **2013**, *5*, 940−948.

(14) Yip, H. L.; Zou, J. Y.; Ma, H.; Tian, Y. Q.; Tucker, N. M.; Jen, A. K. Y. Patterning of robust self-assembled n-type hexaazatrinaphthylene-based nanorods and nanowires by microcontact printing. *J. Am. Chem. Soc.* **2006**, *128*, 13042−13043.

(15) Diegelmann, S. R.; Hartman, N.; Markovic, N.; Tovar, J. D. Synthesis and Alignment of Discrete Polydiacetylene-Peptide Nanostructures. *J. Am. Chem. Soc.* **2012**, *134*, 2028−2031.

(16) Diegelmann, S. R.; Tovar, J. D. Polydiacetylene-Peptide 1D Nanomaterials. *Macromol. Rapid Commun.* **2013**, *34*, 1343−1350.

(17) Volinsky, R.; Gaboriaud, F.; Berman, A.; Jelinek, R. Morphology and organization of phospholipid/diacetylene Langmuir films studied by Brewster angle microscopy and fluorescence microscopy. *J. Phys. Chem. B* **2002**, *106*, 9231−9236.

(18) Gaboriaud, F.; Volinsky, R.; Berman, A.; Jelinek, R. Temperature dependence of the organization and molecular interactions within phospholipid/diacetylene Langmuir films. *J. Colloid Interface Sci.* **2005**, *287*, 191−197.

(19) Huo, Q.; Wang, S. P.; Pisseloup, A.; Verma, D.; Leblanc, R. M. Unusual chromatic properties observed from polymerized dipeptide diacetylenes. *Chem. Commun.* **1999**, 1601−1602.

(20) Lifshitz, Y.; Golan, Y.; Konovalov, O.; Berman, A. Structural Transitions in Polydiacetylene Langmuir Films. *Langmuir* **2009**, *25*, 4469−4477.

(21) Koga, T.; Taguchi, T.; Higashi, N. beta-Sheet peptide-assisted polymerization of diacetylene at the air-water interface and thermochromic property. *Polym. J.* **2012**, *44*, 195−199.

(22) Sigal-Batikoff, I.; Konovalov, O.; Singh, A.; Berman, A. Enantioselective Recognition between Polydiacetylene Nucleolipid Monolayers and Complementary Oligonucleotides. *Langmuir* **2010**, *26*, 16424−16433.

(23) Araghi, H. Y.; Paige, M. F. Deposition and Photopolymerization of Phase-Separated Perfluorotetradecanoic Acid-10,12-Pentacosadiynoic Acid Langmuir-Blodgett Mono layer Films. *Langmuir* **2011**, *27*, 10657−10665.

(24) Upcher, A.; Lifshitz, Y.; Zeiri, L.; Golan, Y.; Berman, A. Effect of Metal Cations on Polydiacetylene Langmuir Films. *Langmuir* **2012**, *28*, 4248−4258.

(25) Jiang, H.; Vinod, T. P.; Jelinek, R. Spontaneous Assembly of Extremely Long, Horizontally-Aligned, Conductive Gold Micro-Wires in a Langmuir Monolayer Template. *Adv. Mater. Interfaces* **2014**, *1*, 6.

(26) Jiang, H.; Jelinek, R. Dramatic Shape Modulation of Surfactant/Diacetylene Microstructures at the Air-Water Interface. *Chem.—Eur. J.* **2014**, *20*, 16747−16752.

(27) Barbera, J.; Puig, L.; Romero, P.; Serrano, J. L.; Sierra, T. Propeller-like hydrogen-bonded banana-melamine complexes inducing helical supramolecular organizations. *J. Am. Chem. Soc.* **2006**, *128*, 4487−4492.

DOI: 10.1021/acs.langmuir.5b01697
Langmuir 2015, 31, 5843−5850

(28) Lio, A.; Reichert, A.; Ahn, D. J.; Nagy, J. O.; Salmeron, M.; Charych, D. H. Molecular imaging of thermochromic carbohydrate-modified polydiacetylene thin films. *Langmuir* **1997**, *13*, 6524−6532.
(29) Gaboriaud, F.; Golan, R.; Volinsky, R.; Berman, A.; Jelinek, R. Organization and structural properties of langmuir films composed of conjugated polydiacetylene and phospholipids. *Langmuir* **2001**, *17*, 3651−3657.
(30) Huang, X.; Li, C.; Jiang, S. G.; Wang, X. S.; Zhang, B. W.; Liu, M. H. Self-assembled spiral nanoarchitecture and supramolecular chirality in Langmuir-Blodgett films of an achiral amphiphilic barbituric acid. *J. Am. Chem. Soc.* **2004**, *126*, 1322−1323.
(31) Jiang, H.; Pan, X. J.; Lei, Z. Y.; Zou, G.; Zhang, Q. J.; Wang, K. Y. Control of supramolecular chirality for polydiacetylene LB films with the command azobenzene derivative monolayer. *J. Mater. Chem.* **2011**, *21*, 4518−4522.
(32) Yagai, S.; Aonuma, H.; Kikkawa, Y.; Kubota, S.; Karatsu, T.; Kitamura, A.; Mahesh, S.; Ajayaghosh, A. Rational Design of Nanofibers and Nanorings through Complementary Hydrogen-Bonding Interactions of Functional pi Systems. *Chem.—Eur. J.* **2010**, *16*, 8652−8661.
(33) Yagai, S.; Usui, M.; Seki, T.; Murayama, H.; Kikkawa, Y.; Uemura, S.; Karatsu, T.; Kitamura, A.; Asano, A.; Seki, S. Supramolecularly Engineered Perylene Bisimide Assemblies Exhibiting Thermal Transition from Columnar to Multilamellar Structures. *J. Am. Chem. Soc.* **2012**, *134*, 7983−7994.
(34) Mori, T.; Sakakibara, K.; Endo, H.; Akada, M.; Okamoto, K.; Shundo, A.; Lee, M. V.; Ji, Q. M.; Fujisawa, T.; Oka, K.; Matsumoto, M.; Sakai, H.; Abe, M.; Hill, J. P.; Ariga, K. Langmuir Nano-architectonics: One-Touch Fabrication of Regularly Sized Nanodisks at the Air-Water Interface. *Langmuir* **2013**, *29*, 7239−7248.
(35) Tieke, B.; Bloor, D.; Young, R. J. Solid-state polymerization of tricosa-10,12-diynoic acid. *J. Mater. Sci.* **1982**, *17*, 1156−1166.
(36) Lifshitz, Y.; Upcher, A.; Kovalev, A.; Wainstein, D.; Rashkovsky, A.; Zeiri, L.; Golan, Y.; Berman, A. Zinc modified polydiacetylene Langmuir films. *Soft Matter* **2011**, *7*, 9069−9077.
(37) Ngampeungpis, W.; Tumcharern, G.; Pienpinijtham, P.; Sukwattanasinitt, M. Colorimetric UV sensors with tunable sensitivity from diacetylenes. *Dyes Pigments* **2014**, *101*, 103−108.
(38) Kootery, K. P.; Jiang, H.; Kolusheva, S.; Vinod, T. P.; Ritenberg, M.; Zeiri, L.; Volinsky, R.; Malferrari, D.; Galletti, P.; Tagliavini, E.; Jelinek, R. Poly(methyl methacrylate)-Supported Polydiacetylene Films: Unique Chromatic Transitions and Molecular Sensing. *ACS Appl. Mater. Interfaces* **2014**, *6*, 8613−8620.

DOI: 10.1021/acs.langmuir.5b01697
Langmuir 2015, 31, 5843−5850